

Nonclassical light at exceptional points of a quantum \mathcal{PT} -symmetric two-mode system

Jan Peřina Jr.* and Antonín Lukš

*Joint Laboratory of Optics, Faculty of Science, Palacký University,
Czech Republic, 17. listopadu 12, 771 46 Olomouc, Czech Republic*

Joanna K. Kalaga and Wiesław Leoński

*Joint Laboratory of Optics, Faculty of Science, Palacký University,
Czech Republic, 17. listopadu 12, 771 46 Olomouc,
Czech Republic; Quantum Optics and Engineering Division,
Faculty of Physics and Astronomy, University of Zielona Góra,
Prof. Z. Szafrana 4a, 65-516 Zielona Góra, Poland*

Adam Miranowicz

Faculty of Physics, Adam Mickiewicz University, 61-614 Poznań, Poland

A two-mode optical parity-time (\mathcal{PT}) symmetric system, with gain and damping, described by a quantum quadratic Hamiltonian with additional small Kerr-like nonlinear terms, is analyzed from the point of view of nonclassical-light generation. Two kinds of stationary states with different types of (in)stability are revealed. Properties of one of these are related to the presence of semiclassical exceptional points, i.e., exotic degeneracies of the non-Hermitian Hamiltonian describing the studied system without quantum jumps. The evolution of the logarithmic negativity, principal squeezing variances, and sub-shot-noise photon-number correlations, considered as entanglement and non-classicality quantifiers, is analyzed in the approximation of linear-operator corrections to the classical solution. Suitable conditions for nonclassical-light generation are identified in the oscillatory regime, especially at and around exceptional points that considerably enhance the nonlinear interaction and, thus, the non-classicality of the generated light. The role of quantum fluctuations, inevitably accompanying attenuation and amplification in the evolution of quantum states, is elucidated. The evolution of the system is analyzed for different initial conditions.

I. INTRODUCTION

Parity-time (\mathcal{PT}) symmetric Hamiltonians have attracted a great deal of attention after the occurrence of the paper by Bender and Boettcher [1–3] in which they showed how such Hamiltonians can be applied for describing physical systems. We note that Hamiltonian \hat{H} is considered to be \mathcal{PT} -symmetric if it is invariant under the combined action of the parity \hat{P} and the time-reversal \hat{T} operators (i.e., \hat{H} commutes with the $\hat{P}\hat{T}$ operator.) Such Hamiltonians, although involving damping and amplification, are endowed with real eigenvalues in certain ranges of their parameters [4]. This is so due to certain balance between the damping and amplification and other parameters describing an open quantum system. Such Hamiltonians have been successfully used for describing numerous classical physical systems involving optical coupled structures [5–8], optical waveguides [9, 10], optical lattices [11–14], coupled optical microresonators [15–19], quantum-electrodynamics circuits (QED) [20], optomechanical systems [21, 22], systems with complex potentials [23], photonics molecules [24], etc. Enhanced sensing in such systems has been demonstrated [17, 25]. Also \mathcal{PT} -symmetric chaotic systems [26–28] and systems exhibiting bidirectional invisibility [29] have been addressed.

Balance between damping and amplification leads, among others, to considerable effective enhancement of both linear and nonlinear interactions in physical systems for suitable parameters, especially at and around exceptional points (EPs) [30, 31]. This is appealing for quantum physicists as it may result in the enhancement of nonclassical behavior of such systems. Here, the question arises what is the counterpart of classical \mathcal{PT} -symmetric Hamiltonians in quantum physics [32–37] and how they behave. The crucial problem here is the conservation of commutation relations among the field operators that is disturbed by the processes of both damping and amplification. The fluctuation-dissipation theorem tells us that both damping and amplification are accompanied by fluctuating forces that affect an analyzed system [35]. Whereas damping and amplification can compensate (equilibrate) each other in the classical evolution, the fluctuating forces related to both of them cannot due to their randomness and quantumness [35]. Especially the noise occurring in the amplification represents a problem [35] that can be circumvented in passive quasi- \mathcal{PT} -symmetric systems [38]. Although the presence of fluctuating forces disturbs the balance between damping and amplification to a certain extent, the enhancement of interactions remains. Strong effective nonlinear interactions can then be used to support the generation of nonclassical light [33, 34]. Moreover, other purely quantum effects have been predicted in quantum \mathcal{PT} -symmetric systems including the generation of en-

* jan.perina.jr@upol.cz

tanglement [39] and the quantum Zeno effect [40]. Also their application in quantum-information processing has been discussed in Ref. [41].

The main goal of this work is the analysis of nonclassical properties of light generated in a typical two-mode \mathcal{PT} -symmetric system with the emphasis on their improvement due to the enhancement of nonlinear interactions in the vicinity of EPs. Here we study the standard (i.e., semiclassical) EPs, corresponding to \mathcal{PT} phase transitions, which are degeneracies of non-Hermitian Hamiltonians describing effectively the system in its semiclassical regime (i.e., without quantum jumps). The motivation for this goal is a rapidly growing research interest and progress, both theoretical and experimental, on EPs in the last decade, as summarized in two recent reviews [30, 31]. This interest has been stimulated by the observation of nontrivial and often counter-intuitive optical and condensed-matter phenomena in the vicinity of EPs, together with the enhancement of interactions. These phenomena can be used to enhance light-matter interactions, as well as to control the generation, transfer, and detection of light. These EP-induced effects include: enhancement of sensing [17, 25, 42], loss-induced photon [16, 43, 44] and phonon [45, 46] lasing, nonreciprocal light transmission [15, 44], unidirectional invisibility [47, 48], chiral modes and directional lasing [49], lasing with enhanced-mode selectivity [50, 51], asymmetric mode switching [52], group velocity control via optomechanically-induced transparency [53], and enhanced optomechanical cooling [54], among many other effects. Applications of EPs are not limited to standard photonics, but also have been proposed for, e.g., microwave photonics using superconducting quantum circuits [20], quantum plasmonics [55] (for a review see [56]), electronics [57, 58], metamaterials [59], cavity optomechanics [45, 54, 60], and acoustics [61, 62]. The EPs, which correspond to \mathcal{PT} phase transitions, are useful to reveal and describe dynamical phase transitions in condensed-matter open quantum systems and to classify their topological phases [63–70] or topological energy transfers [71]. Inspired by these various applications of EPs in the vast majority of semiclassical systems, we now study the behavior of a typical purely quantum \mathcal{PT} -symmetric system at and around EPs.

Although we consider a typical quantum-optical \mathcal{PT} -symmetric system composed of two optical modes, the underlying dynamical operator equations and the resulting behavior are relevant for effective description of analogous systems including matter-field interactions and discussed in some of the above references in the semiclassical approach. Two considered optical modes, one damped and the other amplified, interact via the linear coupling (for scrutinizing the results, see Ref. [72]). A Kerr-type nonlinearity, typical for physical \mathcal{PT} -symmetric systems and originating, e.g., in the gain saturation, is assumed in both modes [33, 34]. Nonclassical behavior of the analyzed system that stems from the Kerr nonlinearity is accompanied by that originating in parametric down-

conversion [73, 74]. Whereas the role of parametric down-conversion in nonclassical-light generation dominates for lower field intensities, the Kerr nonlinearity gives considerable contribution to nonclassical properties at higher field intensities.

In optics, such models comprising two mutually linearly interacting Kerr nonlinear oscillators are referred to as the Kerr couplers [75, 76]. In their usual form of application, i.e. without considering mode amplification and even its balance with damping, they already allow for the observation of squeezing and antibunching as well as the generation of quantum entanglement [77]. Such quantum Kerr oscillators, as nonlinear systems, also exhibit quantum chaotic behavior under suitable conditions [78–82]. When analyzed at the single-photon level, the so-called photon (phonon) blockade effects may occur in the Kerr coupled systems. They result in truncation of the Hilbert space (nonlinear quantum scissors) [83–86] and subsequent generation of highly entangled states [77, 84, 87]. Various forms of quantum correlations such as the entanglement and Einstein-Podolsky-Rosen (EPR) steering were also predicted in short chains of quantum Kerr oscillators [88–91]. On the other hand, the process of parametric down-conversion analyzed alone without any damping or amplification gives rise to both single-mode squeezing and entanglement between both modes expressed through sub-shot-noise photon-number correlations [92].

In our quantum \mathcal{PT} -symmetric model, parametric down-conversion is treated exactly, contrary to the Kerr nonlinearity that is incorporated by using linear-operator corrections to the classical solution obtained for mean values. Properties of steady states including their stability are related to the presence of EPs. In our analysis, we focus on the region with oscillations in the evolution, where real eigenvalues of the Hamiltonian are found and which is the most promising for nonclassical-light generation. EPs lie at the border of this region and provide the greatest effective enhancement of nonlinear interactions. The analysis of similar systems in the regime with amplification, in which complex eigenvalues occur, can be found in Refs. [33, 34] including squeezed-light generation. The oscillatory regime with \mathcal{PT} -symmetry may also be broken due to larger mode intensities, as shown in Ref. [93] by numerical simulations of a classical nonlinear evolution.

The paper is organized as follows. In Sec. II, we introduce the model and find its solution in the approximation of linear-operator corrections to the classical solution. Also entanglement and non-classicality quantifiers used in the analysis are introduced and determined in Sec. II. Steady states of the corresponding classical nonlinear equations and their stability are discussed in Sec. III. Section IV brings the analytical solution of the simplified model that includes just the linear coupling between modes and parametric down-conversion as the source of non-classicality and entanglement. The evolution of quantum states, including the effect of entangle-

ment sudden death and rebirth, is discussed in general in Sec. V. Section VI is devoted to the generation of quantum states at EPs. Finally, Sec. VII brings conclusions. In Appendix A, stability analysis of steady states is given.

II. TWO-MODE \mathcal{PT} -SYMMETRIC SYSTEM WITH PARAMETRIC DOWN-CONVERSION AND ITS QUANTUM EVOLUTION

A. Hamiltonian

We consider a quantum system composed of two optical oscillator modes, labelled as 1 and 2, with identical frequencies ω described by the following Hamiltonian \hat{H} written in the interaction representation [94]:

$$\hat{H} = -i\gamma_1 \hat{a}_1^\dagger \hat{a}_1 - i\gamma_2 \hat{a}_2^\dagger \hat{a}_2 + \left[\epsilon \hat{a}_1^\dagger \hat{a}_2 + \kappa \hat{a}_1 \hat{a}_2 + \text{h.c.} \right] + \beta_1 \hat{a}_1^{\dagger 2} \hat{a}_1^2 + \beta_2 \hat{a}_2^{\dagger 2} \hat{a}_2^2 + \beta_c \hat{a}_1^\dagger \hat{a}_2^\dagger \hat{a}_1 \hat{a}_2. \quad (1)$$

In Eq. (1), symbol \hat{a}_j (\hat{a}_j^\dagger) stands for the annihilation (creation) operator of a photon in mode j , $j = 1, 2$, and h.c. replaces the Hermitian conjugated terms. Whereas mode 1 dissipates with the rate $\gamma_1 \geq 0$, mode 2 is amplified at the rate $-\gamma_2 \geq 0$. Both modes are linearly connected via the coupling constants ϵ and κ . The coupling constant ϵ describes the exchange of photons between both modes, that conserves the energy. It originates, e.g., in the overlap of evanescent waves of wave-guided fields. On the other hand, the coupling constant κ characterizes parametric down-conversion with the simultaneous creation (or annihilation) of two photons, one in mode 1, the other in mode 2. This constant, that quantifies adding or removing the energy in/from the system, is responsible for nonclassical behavior. We note that this term also usually occurs in QED Hamiltonians when non-rotating-wave-approximation (non-RWA) solutions are considered [20]. Moreover, also small Kerr nonlinear terms with nonlinear coupling constants β_1 and β_2 appropriate for modes 1 and 2, respectively, as well as a small cross-Kerr nonlinear term (β_c) are written in Hamiltonian \hat{H} in Eq. (1). These Kerr terms occur naturally in nonlinear photonic structures [73] and also when an optical field interacts with two-level atoms to experience damping or amplification [95].

A \mathcal{PT} -symmetric form of Hamiltonian \hat{H} written in Eq. (1) requires that the exchange of operators of modes 1 and 2 in Eq. (1) transforms the Hamiltonian \hat{H} into its Hermitian conjugated operator \hat{H}^\dagger . This occurs provided that all constants appearing in Eq. (1) are real and

$$\gamma_2 = -\gamma_1, \quad \beta_2 = \beta_1. \quad (2)$$

Moreover, to be useful in physics, the \mathcal{PT} -symmetric form of Hamiltonian \hat{H} should have real eigenvalues [see the condition in Eq. (6) below]. We note that the role of quantum noise in nonlinear evolution of the system under the conditions in Eq. (2) and $\kappa = 0$ was addressed in [36].

B. Heisenberg approach without Langevin forces

To analyze the dynamics of the considered system, we invoke the usual canonical commutation relations for field operators [96] and derive the Heisenberg equations from Hamiltonian \hat{H} in Eq. (1):

$$\begin{aligned} \frac{d\hat{a}_1}{dt} &= -\gamma_1 \hat{a}_1 - i\epsilon \hat{a}_2 - i\kappa \hat{a}_2^\dagger - i\beta_c \hat{a}_2^\dagger \hat{a}_2 \hat{a}_1 - 2i\beta_1 \hat{a}_1^\dagger \hat{a}_1^2, \\ \frac{d\hat{a}_2}{dt} &= -\gamma_2 \hat{a}_2 - i\epsilon \hat{a}_1 - i\kappa \hat{a}_1^\dagger - i\beta_c \hat{a}_1^\dagger \hat{a}_1 \hat{a}_2 - 2i\beta_2 \hat{a}_2^\dagger \hat{a}_2^2, \end{aligned} \quad (3)$$

together with the Hermitian-conjugated ones. However, the solution of the operator equations in the form of Eq. (3) does not conserve the commutation relations because of the damping and amplification terms. To overcome this problem, we have to include the additional fluctuating Langevin operator forces with suitable properties [see Eqs. (9) and (10) and the text below] [32, 36, 94].

Neglecting small nonlinear terms in Eqs. (3) ($\beta_1 = \beta_2 = \beta_c = 0$), we arrive at the following system of linear differential operator equations with constant coefficients:

$$\frac{d}{dt} \begin{bmatrix} \hat{a}_1(t) \\ \hat{a}_1^\dagger(t) \\ \hat{a}_2(t) \\ \hat{a}_2^\dagger(t) \end{bmatrix} = -i \begin{bmatrix} -i\gamma_1 & 0 & \epsilon & \kappa \\ 0 & -i\gamma_1 & -\kappa & -\epsilon \\ \epsilon & \kappa & -i\gamma_2 & 0 \\ -\kappa & -\epsilon & 0 & -i\gamma_2 \end{bmatrix} \begin{bmatrix} \hat{a}_1(t) \\ \hat{a}_1^\dagger(t) \\ \hat{a}_2(t) \\ \hat{a}_2^\dagger(t) \end{bmatrix}. \quad (4)$$

Algebraic analysis of the dynamical matrix of Eq. (4) results in two doubly degenerate eigenfrequencies $\bar{\nu}_{1,2}$:

$$\bar{\nu}_{1,2} = -\frac{i}{2}(\gamma_1 + \gamma_2) \pm \sqrt{\epsilon^2 - \kappa^2 - \frac{(\gamma_1 - \gamma_2)^2}{4}}. \quad (5)$$

According to Eq. (5), real frequencies occur provided that $\gamma_2 = -\gamma_1 \equiv -\gamma$ and

$$\mu^2 \equiv \epsilon^2 - \kappa^2 - \gamma^2 \geq 0. \quad (6)$$

In this case, the eigenvectors $\bar{Y}_{\nu_j}^\pm$ belonging to the doubly degenerate eigenfrequencies $\bar{\nu}_j$, $j = 1, 2$, can be derived in the following form:

$$\begin{aligned} \bar{Y}_{\nu_1}^\pm &= \frac{1}{2\sqrt{\epsilon}} \left(\zeta^\pm, -\zeta^\mp, \pm \frac{\zeta^\pm(\mu + i\gamma)}{\xi}, \mp \frac{\zeta^\mp(\mu + i\gamma)}{\xi} \right), \\ \bar{Y}_{\nu_2}^\pm &= \frac{1}{2\sqrt{\epsilon}} \left(\zeta^\pm, -\zeta^\mp, \mp \frac{\zeta^\pm(\mu - i\gamma)}{\xi}, \pm \frac{\zeta^\mp(\mu - i\gamma)}{\xi} \right) \end{aligned} \quad (7)$$

where $\xi = \sqrt{\epsilon^2 - \kappa^2}$, $\zeta^\pm = \sqrt{\epsilon \pm \xi}$, and $\mu = \sqrt{\xi^2 - \gamma^2}$. Equality in Eq. (6) identifies semiclassical EPs [1] that form the boundary in the space of parameters. For the EPs, the eigenvectors belonging in Eq. (7) to different eigenfrequencies coincide, i.e. $\bar{Y}_{\nu_1}^\pm = \bar{Y}_{\nu_2}^\pm$. We note that Eq. (3) does not include quantum Langevin forces. Thus, the calculated EPs are semiclassical, which might be completely different from quantum EPs related to the Liouvillians, except for the special case of the Hamiltonian in Eq. (1) with $\epsilon > 0$ and $\kappa = \beta_1 = \beta_2 = \beta_c = 0$.

Indeed, as shown in Ref. [37], in this case the quantum and semiclassical EPs are essentially equivalent for larger excitations.

The corresponding classical equations are written for complex amplitudes α_1 and α_2 of fields (in the coherent states $|\alpha_1\rangle$ and $|\alpha_2\rangle$) in modes 1 and 2, respectively:

$$\begin{aligned}\frac{d\alpha_1}{dt} &= -\gamma_1\alpha_1 - i\epsilon\alpha_2 - i\kappa\alpha_2^* - i[\beta_c|\alpha_2|^2 + 2\beta_1|\alpha_1|^2]\alpha_1, \\ \frac{d\alpha_2}{dt} &= -\gamma_2\alpha_2 - i\epsilon\alpha_1 - i\kappa\alpha_1^* - i[\beta_c|\alpha_1|^2 + 2\beta_2|\alpha_2|^2]\alpha_2.\end{aligned}\quad (8)$$

These equations allow in general only for numerical solution.

C. Langevin-Heisenberg approach for quantum amplitude corrections

To solve the nonlinear operator equations in Eq. (3), we adopt the method of linear-operator corrections to the classical solution. Some of the quantum features of the evolving states are then described by the equations for the operator-amplitude corrections $\delta\hat{a}_j$, $j = 1, 2$, to the classical solution ($\hat{a}_j = \alpha_j + \delta\hat{a}_j$). For the Hamiltonian in Eq. (1), they attain the form:

$$\begin{aligned}\frac{d\delta\hat{a}_1}{dt} &= -(\gamma_1 + 4i\beta_1|\alpha_1|^2 + i\beta_c|\alpha_2|^2)\delta\hat{a}_1 - 2i\beta_1|\alpha_1|^2\delta\hat{a}_1^\dagger \\ &\quad - i(\epsilon + \beta_c\alpha_1\alpha_2^*)\delta\hat{a}_2 - i(\kappa + \beta_c\alpha_1\alpha_2)\delta\hat{a}_2^\dagger + \hat{l}_1, \\ \frac{d\delta\hat{a}_2}{dt} &= -i(\epsilon + \beta_c\alpha_1^*\alpha_2)\delta\hat{a}_1 - i(\kappa + \beta_c\alpha_1\alpha_2)\delta\hat{a}_1^\dagger \\ &\quad - (\gamma_2 + 4i\beta_2|\alpha_2|^2 + i\beta_c|\alpha_1|^2)\delta\hat{a}_2 - 2i\beta_2|\alpha_2|^2\delta\hat{a}_2^\dagger \\ &\quad + \hat{l}_2.\end{aligned}\quad (9)$$

The newly introduced fluctuating Langevin operator forces l_1 and l_2 independently compensate for the damping in mode 1 and the amplification in mode 2. We assume their statistical properties in the Markov and Gaussian form [32, 36, 96]:

$$\begin{aligned}\langle \hat{l}_1^\dagger(t)\hat{l}_1(t') \rangle &= 0, \quad \langle \hat{l}_1(t)\hat{l}_1^\dagger(t') \rangle = 2\gamma_1\delta(t-t'), \\ \langle \hat{l}_2^\dagger(t)\hat{l}_2(t') \rangle &= -2\gamma_2\delta(t-t'), \quad \langle \hat{l}_2(t)\hat{l}_2^\dagger(t') \rangle = 0,\end{aligned}\quad (10)$$

where δ stands for the Dirac function.

Equations (9) together with those for the Hermitian-conjugated operator amplitude corrections $\delta\hat{a}_j^\dagger$, $j = 1, 2$, represent a closed set of four linear operator equations having the following matrix form:

$$\frac{d\delta\hat{\mathbf{A}}(t)}{dt} = \mathbf{M}(t)\delta\hat{\mathbf{A}}(t) + \hat{\mathbf{L}}(t), \quad (11)$$

where $\delta\hat{\mathbf{A}}^\text{T} \equiv (\delta\hat{a}_1, \delta\hat{a}_1^\dagger, \delta\hat{a}_2, \delta\hat{a}_2^\dagger)$, $\hat{\mathbf{L}}^\text{T} \equiv (\hat{l}_1, \hat{l}_1^\dagger, \hat{l}_2, \hat{l}_2^\dagger)$, and \mathbf{M} is the appropriate matrix. The solution of Eq. (11) is written as [75]:

$$\delta\hat{\mathbf{A}}(t) = \mathbf{P}(t, 0)\delta\hat{\mathbf{A}}(0) + \hat{\mathbf{F}}(t), \quad (12)$$

$$\hat{\mathbf{F}}(t) = \int_0^t d\tilde{t}\mathbf{P}(t, \tilde{t})\hat{\mathbf{L}}(\tilde{t}). \quad (13)$$

The evolution matrix $\mathbf{P}(t, t')$ is obtained as a solution of the equation

$$d\mathbf{P}(t, t')/dt = M(t)\mathbf{P}(t, t') \quad (14)$$

assuming $\mathbf{P}(t', t')$ is the unity matrix. The correlation functions of the fluctuating operator forces $\hat{\mathbf{F}}(t)$ defined in Eq. (13) are derived from those in Eq. (10) using the formula [75]:

$$\langle \hat{\mathbf{F}}(t)\hat{\mathbf{F}}^\text{T}(t') \rangle = \int_0^t d\tilde{t} \int_0^{t'} d\tilde{t}' \mathbf{P}(t, \tilde{t})(\hat{\mathbf{L}}(\tilde{t})\hat{\mathbf{L}}^\text{T}(\tilde{t}'))\mathbf{P}^\text{T}(t', \tilde{t}'). \quad (15)$$

Using Eq. (12), we express the solution of Eq. (9) for the original operator amplitude corrections in the simplified form:

$$\delta\hat{\mathbf{a}}(t) = \mathbf{U}(t)\delta\hat{\mathbf{a}}(0) + \mathbf{V}(t)\delta\hat{\mathbf{a}}^\dagger(0) + \hat{\mathbf{f}}(t), \quad (16)$$

where $\delta\hat{\mathbf{a}}^\text{T} \equiv (\delta\hat{a}_1, \delta\hat{a}_2)$, $U_{j,k}(t) = P_{2j-1, 2k-1}(t, 0)$, $V_{jk}(t) = P_{2j-1, 2k}(t, 0)$, and $\hat{f}_j(t) = \hat{F}_{2j-1}(t)$, $j, k = 1, 2$.

In our analysis, in which we assume incident vacuum or coherent states, the generated states remain Gaussian and so we express their normal characteristic function $C_{\mathcal{N}}$ as [94]

$$\begin{aligned}C_{\mathcal{N}}(\mu_1, \mu_2, t) &= \exp \left\{ \sum_{j=1,2} \left[(\alpha_j^*(t)\mu_j - \text{c.c.}) \right. \right. \\ &\quad \left. \left. - B_j(t)|\mu_j|^2 + (C_j(t)\mu_j^{2*} - \text{c.c.})/2 \right] \right. \\ &\quad \left. + (D(t)\mu_1^*\mu_2^* + \bar{D}(t)\mu_1\mu_2 + \text{c.c.}) \right\},\end{aligned}\quad (17)$$

where c.c. replaces the complex-conjugated term. The functions B_j , C_j ($j = 1, 2$), D , and \bar{D} introduced in Eq. (17) are given for the incident coherent states as:

$$\begin{aligned}B_j(t) &\equiv \langle \delta\hat{a}_j^\dagger(t)\delta\hat{a}_j(t) \rangle = \sum_{l=1,2} \left[|V_{jl}(t)|^2 + \langle \hat{f}_j^\dagger(t)\hat{f}_j(t) \rangle \right], \\ C_j(t) &\equiv \langle [\delta\hat{a}_j(t)]^2 \rangle = \sum_{l=1,2} \left[U_{jl}(t)V_{jl}(t) + \langle \hat{f}_j(t) \rangle^2 \right], \\ D(t) &\equiv \langle \delta\hat{a}_1(t)\delta\hat{a}_2(t) \rangle \\ &= \sum_{l=1,2} \left[U_{1l}(t)V_{2l}(t) + \langle \hat{f}_1(t)\hat{f}_2(t) \rangle \right], \\ \bar{D}(t) &\equiv -\langle \delta\hat{a}_1^\dagger(t)\delta\hat{a}_2^\dagger(t) \rangle \\ &= -\sum_{l=1,2} \left[V_{1l}^*(t)V_{2l}(t) + \langle \hat{f}_1^\dagger(t)\hat{f}_2^\dagger(t) \rangle \right].\end{aligned}\quad (18)$$

As the functions D and \bar{D} occur in the characteristic function $C_{\mathcal{N}}$ in Eq. (18), the described state may exhibit entanglement. It can be quantified via the logarithmic negativity $E_{\mathcal{N}}$ determined from the symmetric covariance matrix as described in Ref. [97]. This entanglement may lead to quantum correlations between the photon numbers n_1 and n_2 of both modes. These correlations are usually quantified by the sub-shot-noise parameter

$R < 1$ where $R \equiv \langle \Delta(\hat{n}_1 - \hat{n}_2)^2 \rangle / (\langle \hat{n}_1 \rangle + \langle \hat{n}_2 \rangle)$, $\hat{n}_j = \hat{a}_j^\dagger \hat{a}_j$, $j = 1, 2$ and $\Delta \hat{x} = \hat{x} - \langle \hat{x} \rangle$ for an arbitrary operator \hat{x} . For the characteristic function $C_{\mathcal{N}}$ in Eq. (17) with the coefficients in Eq. (18), the sub-shot-noise parameter R attains the form:

$$R = 1 + \left\{ \sum_{j=1,2} [b_j^2 + |c_j|^2] - 2|d|^2 - 2|\bar{d}|^2 - 2(|\alpha_1|^2 - |\alpha_2|^2)^2 \right\} / (b_1 + b_2) \quad (19)$$

and $b_j = |\alpha_j|^2 + B_j$, $c_j = \alpha_j^2 + C_j$ ($j = 1, 2$), $d = \alpha_1 \alpha_2 + D$, and $\bar{d} = \alpha_1^* \alpha_2 - \bar{D}$.

The generated states exhibit their non-classicality also as the squeezing of phase fluctuations of their complex amplitudes. Both single-mode squeezing quantified by the principal squeezing variances λ_1 and λ_2 smaller than 1 [98] and two-mode squeezing described by the principal squeezing variance $\lambda < 2$ [94] may be observed:

$$\lambda_j = 1 + 2(B_j - |C_j|), \quad j = 1, 2, \quad (20)$$

$$\lambda = 1 + 2(B_1 + B_2 - \bar{D} - \bar{D}^* - |C_1 + C_2 + 2D|). \quad (21)$$

III. STEADY STATES AND THEIR STABILITY ANALYSIS

For the general form of Hamiltonian \hat{H} in Eq. (1), we find two nontrivial steady states and analyze their stability. Expressing the complex amplitudes α_j as $\varrho_j \exp(i\varphi_j)$, $j = 1, 2$, we transform the nonlinear equations in Eq. (3) into the form:

$$\begin{aligned} \frac{d\varrho_1}{dt} &= -\gamma_1 \varrho_1 + [\epsilon \sin(\varphi) - \kappa \sin(\psi)] \varrho_2, \\ \frac{d\varrho_2}{dt} &= -\gamma_2 \varrho_2 - [\epsilon \sin(\varphi) + \kappa \sin(\psi)] \varrho_1, \\ \frac{d\varphi_1}{dt} &= -[\epsilon \cos(\varphi) + \kappa \cos(\psi)] \frac{\varrho_2}{\varrho_1} - \beta_c \varrho_2^2 - 2\beta_1 \varrho_1^2, \\ \frac{d\varphi_2}{dt} &= -[\epsilon \cos(\varphi) + \kappa \cos(\psi)] \frac{\varrho_1}{\varrho_2} - \beta_c \varrho_1^2 - 2\beta_2 \varrho_2^2, \end{aligned} \quad (22)$$

where $\psi = \varphi_2 + \varphi_1$ and $\varphi = \varphi_2 - \varphi_1$.

To reveal steady states of Eqs. (22), we set

$$\frac{d\varrho_1}{dt} = \frac{d\varrho_2}{dt} = \frac{d\varphi_1}{dt} = \frac{d\varphi_2}{dt} = 0. \quad (23)$$

The subtraction of the fourth equation multiplied by ϱ_1^2 from the third one multiplied by ϱ_2^2 leads us to the relation between the amplitudes ϱ_1 and ϱ_2 :

$$\varrho_2^{\text{st}} = \beta_{12} \varrho_1^{\text{st}}, \quad (24)$$

where $\beta_{12} \equiv \sqrt[4]{\beta_1/\beta_2}$ (we assume $\beta_1, \beta_2 > 0$). For the steady states and their stability analysis in the special case in which only the cross-Kerr nonlinearity is present ($\beta_1 = \beta_2 = 0$, $\beta_c \neq 0$), see Ref. [99].

Using this relation, the first and second equations in Eqs. (22) are transformed into the form:

$$\begin{aligned} \gamma_2 \beta_{12} &= -\epsilon \sin(\varphi^{\text{st}}) - \kappa \sin(\psi^{\text{st}}), \\ \gamma_1 / \beta_{12} &= \epsilon \sin(\varphi^{\text{st}}) - \kappa \sin(\psi^{\text{st}}). \end{aligned} \quad (25)$$

The solution of the linear algebraic equations in Eq. (25) with respect to $\sin(\varphi^{\text{st}})$ and $\sin(\psi^{\text{st}})$ leaves us with the formulas for angles φ^{st} and ψ^{st} :

$$\begin{aligned} \psi^{\text{st}} &= \arcsin \left[\frac{-\gamma_2 \beta_{12} - \gamma_1 / \beta_{12}}{2\kappa} \right], \\ \varphi^{\text{st}} &= \arcsin \left[\frac{-\gamma_2 \beta_{12} + \gamma_1 / \beta_{12}}{2\epsilon} \right]. \end{aligned} \quad (26)$$

Finally, applying Eq. (24) in the third equation in Eqs. (22) we arrive at the formula for ϱ_1^{st} (we assume $\beta_c > -2\sqrt{\beta_1\beta_2}$)

$$\varrho_1^{\text{st}} = \sqrt{\frac{-c_\epsilon - c_\kappa}{\beta_c \beta_{12} + 2\beta_1 / \beta_{12}}} \quad (27)$$

that identifies two distinct steady states. We have for the first one

$$c_\epsilon = \mp \epsilon |\cos(\varphi^{\text{st}})| \quad \text{and} \quad c_\kappa = \mp \kappa |\cos(\psi^{\text{st}})|, \quad (28)$$

where the combination of signs has to guarantee that $\varrho_1^{\text{st}} \geq 0$. On the other hand, the second steady state is identified via one combination of signs assuring that $\varrho_1^{\text{st}} \geq 0$:

$$c_\epsilon = \pm \epsilon |\cos(\varphi^{\text{st}})| \quad \text{and} \quad c_\kappa = \mp \kappa |\cos(\psi^{\text{st}})|. \quad (29)$$

A numerical analysis of the first steady state of Eq. (28) reveals the expected physical behavior. The state is stable [unstable] if the damping in the system dominates [is dominated by] its amplification ($\gamma_1 > |\gamma_2|$) [$\gamma_1 < |\gamma_2|$]. For the \mathcal{PT} -symmetric case $\gamma_2 = -\gamma_1$, the frequencies in the stability analysis are real (for the analytical results in this case, see Appendix A).

On the other hand, the second steady state of Eq. (29) is unstable independently of the relation between the values of γ_1 and $|\gamma_2|$. Only in EPs occurring in \mathcal{PT} -symmetric systems, all frequencies in the stability analysis are zero (see Fig. 1). We note that the analyzed EPs are semiclassical, i.e. they belong to open quantum models in their semiclassical limit, where quantum jumps are ignored. In open models with quantum jumps, quantum EPs can be analyzed using the Liouvillian spectra, as recently demonstrated in [37]. In the analyzed semiclassical EPs, the amplitudes ϱ_1^{st} and ϱ_2^{st} of the steady state vanish, i.e., the steady state coincides with the trivial steady state. In our opinion, the presence of such specific steady states in nonlinear systems reveals the same values of parameters as those identified by the linear analysis as EPs [compare Eq. (6)].

If a steady state is considered as the classical solution, the matrix \mathbf{M} of the linear operator equations in Eq. (11) is time independent and the evolution can be

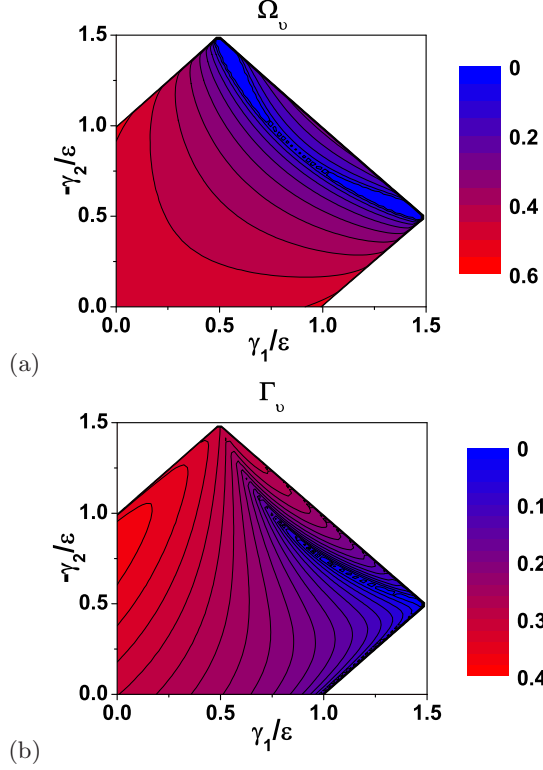


FIG. 1. Maximal values of the real and imaginary parts of four complex frequencies plotted as functions (a) $\Omega_{\tilde{\nu}} = \log[1 + |\text{Re}(\tilde{\nu})|]$ and (b) $\Gamma_{\tilde{\nu}} = \text{sign}[\text{Im}(\tilde{\nu})] \log[1 + |\text{Im}(\tilde{\nu})|]$ depending on the varying dimensionless damping and amplification parameters γ_1/ϵ and $-\gamma_2/\epsilon$; sign gives the sign of its argument, log means the decimal logarithm, $\kappa = 0.5\epsilon$, $\beta_1 = \beta_2 = 0.05\epsilon$, and $\beta_c = 0$.

formulated in terms of its eigenvalues ($-i\tilde{\nu}_j$) and corresponding eigenvectors \mathbf{Y}_j , $j = 1, \dots, 4$. Forming a matrix \mathbf{Y} from the eigenvectors \mathbf{Y}_j placed as columns and introducing the matrix \mathbf{y} as its inverse, we can express the elements of the matrices \mathbf{U} and \mathbf{V} in Eq. (16) and the matrix $\langle \hat{\mathbf{F}} \hat{\mathbf{F}}^T \rangle$ in Eq. (15) as follows:

$$\begin{aligned}
 U_{jk}(t) &= \sum_{l=1}^4 \exp(-i\tilde{\nu}_l t) Y_{2j-1,l} y_{l,2k-1}, \\
 V_{jk}(t) &= \sum_{l=1}^4 \exp(-i\tilde{\nu}_l t) Y_{2j-1,l} y_{l,2k}, \\
 \langle \hat{\mathbf{F}}_k(t) \hat{\mathbf{F}}_{k'}^T(t) \rangle &= 2i \sum_{l,l'=1}^4 Y_{kl} Y_{k'l'} \frac{\exp[-i(\tilde{\nu}_l + \tilde{\nu}_{l'})t] - 1}{\tilde{\nu}_l + \tilde{\nu}_{l'}} \\
 &\quad \times [\gamma_1 y_{l1} y_{l'2} - \gamma_2 y_{l4} y_{l'3}]. \tag{30}
 \end{aligned}$$

IV. PARAMETRIC DOWN-CONVERSION AS THE SOURCE OF NON-CLASSICALITY IN \mathcal{PT} -SYMMETRIC SYSTEM

Before we analyze the behavior of the system under general conditions numerically, we derive analytical formulas for the considered quantities in the most simplified form of Hamiltonian \hat{H} in which only ϵ and κ are nonzero. Zero values of γ_1 and γ_2 mean no fluctuating forces. This analysis provides an insight into the behavior of non-classicality.

In this case, the field operators obey Eq. (4) with $\gamma_1 = \gamma_2 = 0$. Equation (5) gives us two doubly degenerate real eigenfrequencies $\tilde{\nu}_{1,2} = \pm\xi$, $\xi = \sqrt{\epsilon^2 - \kappa^2}$. The solution of the Heisenberg equations is then obtained as

$$\begin{aligned}
 \hat{a}_1(t) &= \cos(\xi t) \hat{a}_1(0) \\
 &\quad - i \sin(\xi t) \left[(\epsilon/\xi) \hat{a}_2(0) + (\kappa/\xi) \hat{a}_2^\dagger(0) \right], \\
 \hat{a}_2(t) &= \cos(\xi t) \hat{a}_2(0) \\
 &\quad - i \sin(\xi t) \left[(\epsilon/\xi) \hat{a}_1(0) + (\kappa/\xi) \hat{a}_1^\dagger(0) \right]. \tag{31}
 \end{aligned}$$

For the solution in Eq. (31), the parameters of the characteristic function C_N defined in Eqs. (18) attain the form:

$$\begin{aligned}
 B_1(t) &= B_2(t) = (\kappa/\xi)^2 \sin^2(\xi t), \\
 C_1(t) &= C_2(t) = -(\epsilon\kappa/\xi^2) \sin^2(\xi t), \\
 D(t) &= -i(\kappa/\xi) \sin(2\xi t)/2, \\
 \bar{D} &= 0. \tag{32}
 \end{aligned}$$

Further, the symmetric covariance matrix \mathbf{C}_S is derived in the following form:

$$\mathbf{C}_S = \begin{bmatrix} 1 + d_1(t) & 0 & 0 & d_3(t) \\ 0 & 1 + d_2(t) & d_3(t) & 0 \\ 0 & d_3(t) & 1 + d_1(t) & 0 \\ d_3(t) & 0 & 0 & 1 + d_2(t) \end{bmatrix}, \tag{33}$$

where $d_1(t) = -[2\kappa/(\epsilon + \kappa)] \sin^2(\xi t)$, $d_2(t) = [2\kappa/(\epsilon - \kappa)] \sin^2(\xi t)$, and $d_3(t) = -[\kappa/\xi] \sin(2\xi t)$. The symplectic eigenvalues σ_\pm of the positive-partial-transposed (PPT) covariance matrix \mathbf{C}_S with $\det(\mathbf{C}_S) = 1$ fulfill $\sigma_\pm^2 = (\Delta \pm \sqrt{\Delta^2 - 4})/2$ [97, 100] where the serialian Δ (the second global invariant of matrices 4×4 , that accompanies the determinant, see, e.g., [97]) is derived as:

$$\Delta = 2 + (2\kappa/\xi)^2 \sin^2(2\xi t). \tag{34}$$

Using these results, the positive logarithmic negativity E_N [97, 100] is determined by the formula $E_N = -\log(\sigma_-^2)/2$ applicable if $|\sigma_-| < 1$:

$$E_N(t) = -\frac{1}{2} \log \left(1 + 2 \frac{1 - \sqrt{1 + g^2(t)}}{g^2(t)} \right) \tag{35}$$

and $g(t) = \xi/[\kappa \sin(2\xi t)]$.

Assuming the incident vacuum states, Eq. (19) provides the sub-shot-noise parameter R as

$$R(t) = 2(\epsilon/\xi)^2 \sin^2(\xi t). \quad (36)$$

The principal squeezing variances, determined along Eqs. (20) and (21), are obtained for arbitrary incident coherent states as:

$$\begin{aligned} \lambda_1(t) &= \lambda_2(t) = 1 - 2[\kappa/(\epsilon + \kappa)] \sin^2(\xi t), \\ \lambda(t) &= 2 \left[1 + 2(\kappa/\xi)^2 \sin^2(\xi t) - 2(\kappa/\xi^2) |\sin(\xi t)| \right. \\ &\quad \left. \times \sqrt{\epsilon^2 - \kappa^2 \cos^2(\xi t)} \right]. \end{aligned} \quad (37)$$

For the semiclassical EP occurring for $\epsilon = \kappa$, the above formulas simplify to

$$\begin{aligned} E_N(t) &= -\frac{1}{2} \log \left(1 + 8\epsilon^2 t^2 - 4\epsilon t \sqrt{1 + 4\epsilon^2 t^2} \right), \\ R(t) &= 2\epsilon^2 t^2, \\ \lambda_1 &= \lambda_2 = 1, \\ \lambda(t) &= 2 \left(1 + 2\epsilon^2 t^2 - 2\epsilon t \sqrt{1 + \epsilon^2 t^2} \right). \end{aligned} \quad (38)$$

According to Eq. (38), the non-classicality is 'encoded' only in the correlations between the modes. Whereas the sub-shot-noise parameter R is nonclassical only for short times, two-mode squeezing gradually develops with time and it becomes maximal for $t \rightarrow \infty$. Except for $t = 0$, the states are entangled and the logarithmic negativity E_N even goes to infinity for $t \rightarrow \infty$.

For a system with general parameters ($\epsilon \neq \kappa$), the maximal value E_N^{\max} of the logarithmic negativity and the minimal values of the sub-shot-noise parameter R^{\min} and the principal squeezing variances ($\lambda_{1,2}^{\min}$, λ^{\min}) taken over $t \in \langle 0, \infty \rangle$ reveal the system potential to generate nonclassical states:

$$\begin{aligned} E_N^{\max} &= -\frac{1}{2} \log \left(\frac{\epsilon - \kappa}{\epsilon + \kappa} \right), \\ R^{\min} &= 0, \\ \lambda_1^{\min} &= \lambda_2^{\min} = \lambda^{\min} / 2 = \frac{\epsilon - \kappa}{\epsilon + \kappa}. \end{aligned} \quad (39)$$

The analysis of formulas in Eq. (39) confirms that the best conditions for the generation of nonclassical states occur at the EP, i.e. if $\epsilon = \kappa$. Moreover, the larger the distance $\epsilon - \kappa$ from the EP in the space of parameters is, the worse the non-classicality parameters are. It is worth noting that the extremal values in Eq. (39) are reached at different time instants: $\xi t = \pi/4 + n\pi$ for E_N^{\max} , $\xi t = \pi/2 + n\pi$ for λ_1^{\min} , λ_2^{\min} and λ^{\min} , and $\xi t = (n+1)\pi$ for R^{\min} , $n = 0, 1, \dots$

V. NONCLASSICAL STATES AND THEIR TIME EVOLUTION

Based on numerical analysis, we extend the discussion of nonclassical properties of the generated states

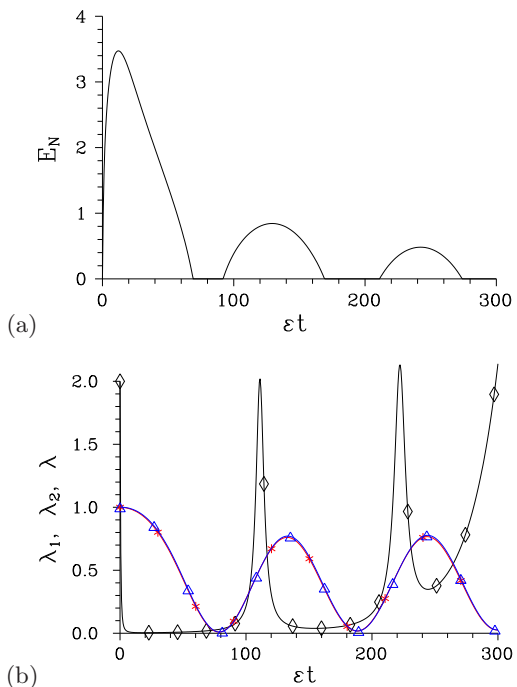


FIG. 2. (a) Logarithmic negativity E_N and (b) principal squeezing variances λ_1 (*), λ_2 (Δ) and λ (\diamond) as they depend on dimensionless time ϵt ; $\gamma = 1 \times 10^{-4}\epsilon$, $\kappa = (1 - 1 \times 10^{-4})\epsilon$, $\beta_1 = \beta_2 = 0.05\epsilon$, and $\beta_c = 0$. The initial steady state in Eq. (29) is assumed.

from Sec. IV to the case with damping and amplification. First, we consider only weak damping and amplification. In this case, the system with parametric down-conversion as a source of non-classicality has enough time to evolve an initial classical state into highly nonclassical states endowed with entanglement, squeezing, and sub-shot-noise photon-number correlations, as shown in Fig. 2. Even, provided that we consider an initial state close to the second stationary state of Eq. (29) we observe the effect of entanglement sudden death and rebirth in the evolution of the logarithmic negativity E_N [see Fig. 2(a)]. A comparison of the curves in Figs. 2(a) and 2(b) reveals that the states exhibit single mode non-classicality evidenced by the single-mode principal squeezing variances λ_1 and λ_2 even at time instants in which the entanglement vanishes. Also, the time evolution of the two-mode principal squeezing variance λ in Fig. 2(b) documents that its nonclassical values may originate either in single-mode non-classicalities or two-mode entanglement. In general, the curves in Fig. 2 show that even small values of damping and amplification result in a gradual loss of non-classicality during the time evolution.

Greater values of damping and amplification naturally lead to a faster loss of non-classicality for two possible reasons. The first reason is the presence of damping and amplification terms in the Heisenberg equations in Eqs. (9), the second one is the presence of fluctuating Langevin forces in Eq. (9) that constantly add the

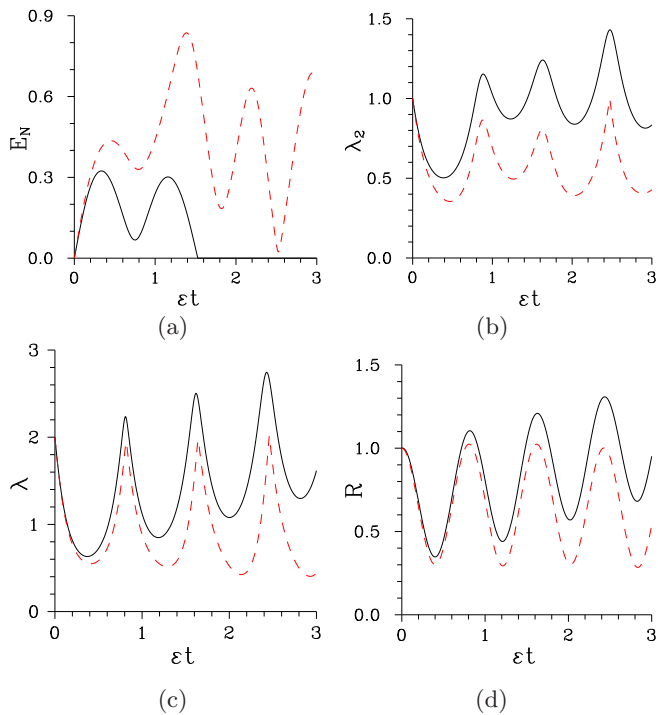


FIG. 3. (a) Logarithmic negativity E_N , (b) principal squeezing variance λ_2 , (c) principal squeezing variance λ , and (d) sub-shot-noise parameter R as they depend on dimensionless time ϵt ; $\gamma = 0.1\epsilon$, $\kappa = 0.9\epsilon$, $\beta_1 = \beta_2 = 0.05\epsilon$, and $\beta_c = 0$. The initial steady state in Eq. (28) is assumed, evolution is treated with [without] the fluctuating Langevin forces (black solid [red dashed] curves).

noise into the state during its evolution. Although both contributions are intimately related by the fluctuation-dissipation theorem [94], we may separate them in our model to judge independently their roles in the state evolution (see Fig. 3). Comparison of the solid and dashed curves in Fig. 3 leads us to the important conclusion that the Langevin forces are dominantly responsible for a gradual loss of non-classicality during the evolution.

Increasing the damping and amplification constants γ_1 and γ_2 in general reduces the system ability to provide nonclassical states. Greater values of the coupling constant κ , that is the source of non-classicality, allow the observation of highly nonclassical states for greater values of the damping and amplification constants γ_1 and γ_2 . According to Fig. 4(a), the logarithmic negativity E_N^{\max} attains its greatest values [the greatest non-classicality] for κ/ϵ close to 1 and γ close to 0 and decreasing (increasing) values of κ (γ) systematically reduce its values [reduce the non-classicality]. From the point of view of non-classicality, the sub-shot-noise parameter R^{\min} and the two-mode principal squeezing variance λ^{\min} behave qualitatively similarly as the logarithmic negativity E_N^{\max} . Also the single-mode principal squeezing variances λ_1^{\min} and λ_2^{\min} reach their smallest values [the greatest non-classicality] in the area with greater κ and small γ , as shown in Figs. 4(b) and 4(c). The comparison

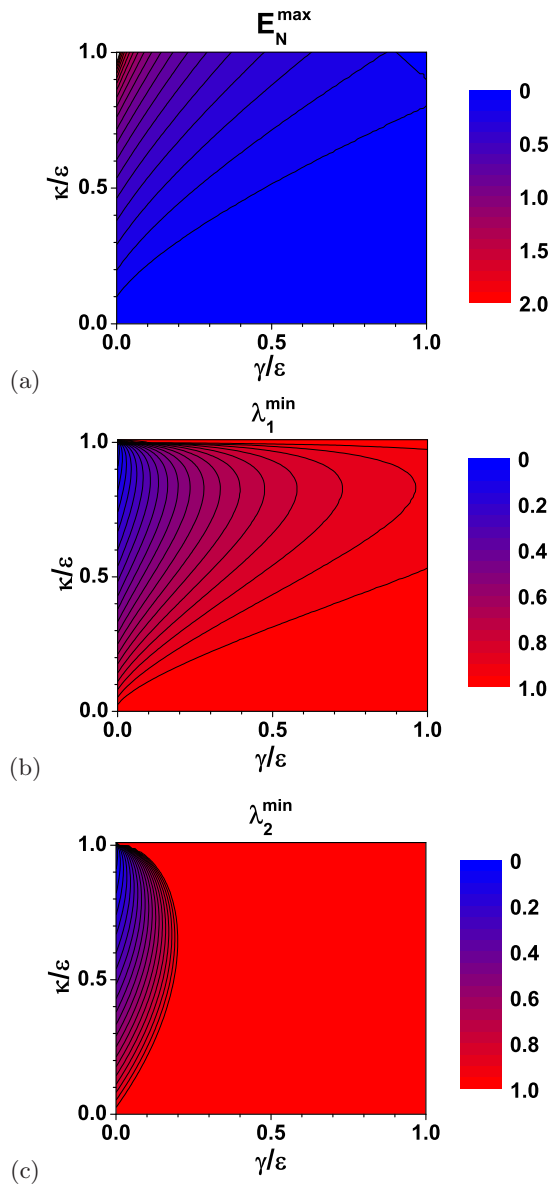


FIG. 4. (a) Logarithmic negativity E_N and principal squeezing variances (b) λ_1 and (c) λ_2 as they depend on dimensionless parameters γ/ϵ and κ/ϵ ; $\beta_1 = \beta_2 = 0.05\epsilon$ and $\beta_c = 0$. The initial vacuum states are assumed.

of Figs. 4(b) and 4(c) confirms our general observation that the single-mode non-classicality develops more extensively in the damped mode 1 rather than in the amplified mode 2.

VI. NONCLASSICAL STATES AT EXCEPTIONAL POINTS

As already discussed in Sec. III, the most promising conditions for the nonclassical-light generation are found in EPs in the parameter space, i.e. if $\epsilon^2 - \kappa^2 - \gamma^2 = 0$ [see Eq. (6)]. This stems from the fact that the interactions

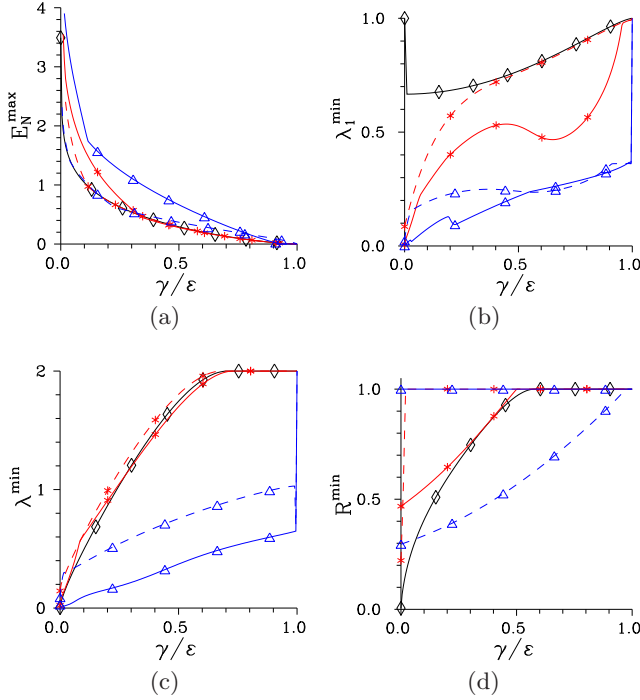


FIG. 5. (a) Logarithmic negativity E_N^{\max} , (b) principal squeezing variance λ_1^{\min} , (c) principal squeezing variance λ^{\min} , and (d) sub-shot-noise parameter R^{\min} as they depend on dimensionless damping and amplification constant γ/ϵ for semiclassical EPs; $\kappa = \sqrt{\epsilon^2 - \gamma^2}$, $\beta_1 = \beta_2 = 0.05\epsilon$, and $\beta_c = 0$. Considered initial states: $\alpha_1^{\text{in}} = \alpha_2^{\text{in}} = 1 \times 10^{-8}$ (solid curves with \diamond), $\alpha_1^{\text{in}} = \alpha_2^{\text{in}} = 1/\sqrt{2}$ $[10/\sqrt{2}]$ (solid curves with \ast $[\triangle]$) and $\alpha_1^{\text{in}} = -\alpha_2^{\text{in}} = -i/\sqrt{2}$ $[-10i/\sqrt{2}]$ (dashed curves with \ast $[\triangle]$).

between modes are enhanced in these points [39]. The ability to generate nonclassical states decreases with the increasing damping and amplification constants γ_1 and γ_2 , as shown in Fig. 5. According to the curves in Fig. 5 drawn for E_N^{\max} , λ_1^{\min} , λ^{\min} , and R^{\min} , greater intensities of the incident coherent states lead to greater values of the logarithmic negativity E_N^{\max} and smaller values of the principal squeezing variances λ_1^{\min} and λ^{\min} . Moreover, they allow for the observation of single- as well as two-mode squeezing in case of strong damping and amplification, which is impossible for initial coherent states close to the vacuum state. The behavior of sub-shot-noise parameter R^{\min} strongly depends on the relative phase of the initial coherent states [see Fig. 5(d)]. If the initial amplitudes are in-phase, the sub-shot-noise photon-number correlations gradually vanish with the increasing mode intensities. On the other hand, if the initial amplitudes are out of phase, the photon-number correlations become nonclassical (R^{\min}) only for greater incident mode intensities.

Nonclassical properties of the generated states depend strongly on initial conditions, namely on the overall initial intensity I^{in} ($I \equiv |\alpha_1|^2 + |\alpha_2|^2$), the initial-intensities unbalance quantified by the angle θ^{in} [$|\alpha_1|^2 = \cos^2(\theta)I$,

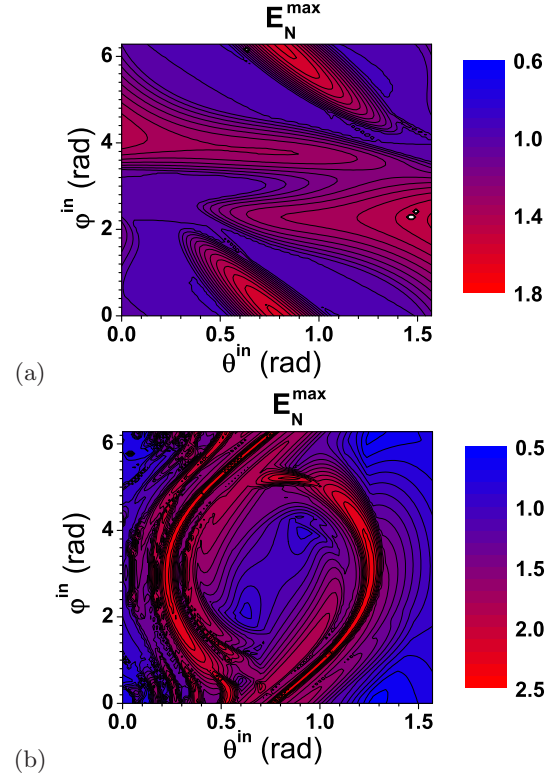


FIG. 6. Logarithmic negativity E_N^{\max} for (a) $I^{\text{in}} = 1$ and (b) $I^{\text{in}} = 100$ as it depends on initial angle θ^{in} giving intensity unbalance and phase difference φ^{in} for $\psi^{\text{in}} = 0$ and the semiclassical EP given as $\gamma/\epsilon = 0.1$, $\kappa = \sqrt{\epsilon^2 - \gamma^2}$; $\beta_1 = \beta_2 = 0.05\epsilon$ and $\beta_c = 0$.

$|\alpha_2|^2 = \sin^2(\theta)I$] and the initial relative phase φ^{in} defined below Eq. (22). We note that strong dependence of the classical solution of the two-mode Kerr system on initial conditions was widely discussed in [93] in relation to \mathcal{PT} -symmetry breaking. As shown in Fig. 6, the patterns giving the logarithmic negativity E_N^{\max} in the plane $(\theta^{\text{in}}, \varphi^{\text{in}})$ qualitatively depend on the overall initial intensity I^{in} .

Whereas the logarithmic negativity E_N^{\max} depends smoothly on the initial-intensities unbalance (θ^{in}) for small intensities I^{in} , its strong dependence is observed for greater intensities I^{in} [compare Figs. 6(a) and 6(b)]. The presence of ring-like structures in Fig. 6(b) reflects stronger influence of the nonlinear Kerr terms to the evolution [the terms with β_1 , β_2 and β_c in Eqs. (3)]. These terms that are weak for small intensities start to play an important role for greater intensities. They, in parallel to those depending on κ , also serve as a source of non-classicality of the generated states. Qualitatively different patterns of sub-shot-noise parameter R^{\min} drawn for small and large intensities I^{in} in Figs. 7(a) and 7(b) confirm the role of Kerr terms in the state evolution and the development of its nonclassical properties. The patterns of the principal squeezing variances λ_1^{\min} , λ_2^{\min} , and λ^{\min} are similarly affected by the initial intensity I^{in} .

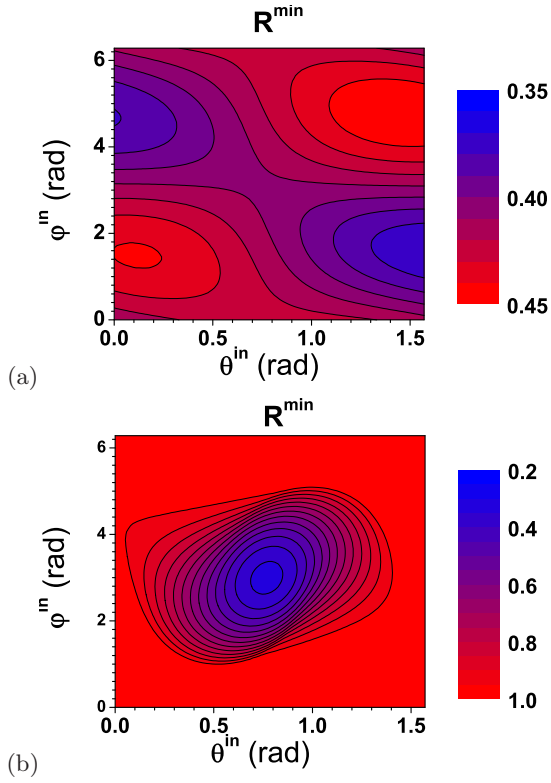


FIG. 7. Sub-shot-noise parameter R^{\min} for (a) $I^{\text{in}} = 1$ and (b) $I^{\text{in}} = 100$ as it depends on initial angle θ^{in} and phase difference φ^{in} for $\psi^{\text{in}} = 0$ and the semiclassical EP specified in the caption to Fig. 6.

VII. CONCLUSIONS

Quantum evolution of a two-mode optical system, described by a quadratic Hamiltonian with additional small nonlinear Kerr terms and exposed to simultaneous damping and amplification, was discussed in the \mathcal{PT} -symmetric configuration. Two kinds of stationary states were revealed for the classical nonlinear equations corresponding to the quantum Heisenberg equations of the analyzed system. Whereas the stationary states of the first kind are stable for damping prevailing the amplification, the stationary states of the second kind are always unstable. The latter states coincide with the vacuum state in EPs. This allows, in principle, to look for the EPs through seeking for the stationary states with specific properties. Quantum consistent evolution of fields in the \mathcal{PT} -symmetric model was formulated using linear-operator corrections to the classical solution that was found in general numerically. In the model, parametric down-conversion with its creation and annihilation of photons in pairs represents the main source of non-classicality of the emitted fields at lower intensities. These fields can exhibit both two-mode entanglement and single-mode non-classicalities. Stronger parametric down-conversion together with weak damping and amplification were shown to be suitable for the generation

of highly nonclassical states judged via the values of the logarithmic negativity, the principal squeezing variances, and the sub-shot-noise parameter. Highly nonclassical states were especially observed at EPs due to the effective enhancement of nonlinearity. It holds in general that the evolution gradually conceals the non-classicality of the evolving states for nonzero damping and amplification. Highly non-classical states are thus obtained for finite time instants. It was shown that the presence of fluctuating Langevin forces (not the sheer presence of damped and amplified terms in the Heisenberg equations) is the main reason for this gradual loss of non-classicality. The analyzed \mathcal{PT} -symmetric system with parametric down-conversion has been revealed as the source of highly non-classical light, especially at EPs with weak damping and amplification. These nonclassical properties represent a challenge for its practical realization in the form of a nonlinear photonic structure.

ACKNOWLEDGMENTS

Acknowledgments J.P. acknowledges the support by the GA ĀR project 18-22102S. J.P., J.K.K., and W.L. were supported from ERDF/ESF project “Nanotechnologies for Future” (CZ.02.1.01/0.0/0.0/16_019/0000754). A.L. gratefully acknowledges the support from the project IGA_PrF_2019_008 of Palacký University. J.K.K. and W.L. acknowledge the financial support from the program of the Polish Minister of Science and Higher Education under the name “Regional Initiative of Excellence” in 2019-2022, project no. 003/RID/2018/19, funding amount 11 936 596.10 PLN.

Appendix A: Stability analysis of steady states

To analyze stability of the steady states revealed in Sec. III and described in Eqs. (28) and (29), we express the used quantities via their deviations $\delta\rho_1$, $\delta\rho_2$, $\delta\varphi$, and $\delta\psi$ from their steady-state values:

$$\begin{aligned} \rho_j &= \rho_j^{\text{st}} + \delta\rho_j, \quad j = 1, 2, \\ \varphi &= \varphi^{\text{st}} + \delta\varphi, \quad \psi = \psi^{\text{st}} + \delta\psi. \end{aligned} \quad (\text{A1})$$

The linearized equations for the deviations are derived as follows:

$$\begin{aligned} \frac{d}{dt} \begin{bmatrix} \delta\rho_1 \\ \delta\rho_2 \\ \delta\varphi \\ \delta\psi \end{bmatrix} &= \begin{bmatrix} \gamma_1 & s_\epsilon - s_\kappa & c_\epsilon \rho_2^{\text{st}} & -c_\kappa \rho_2^{\text{st}} \\ -s_\epsilon - s_\kappa & -\gamma_2 & -c_\epsilon \rho_1^{\text{st}} & -c_\kappa \rho_1^{\text{st}} \\ G^+ & H^+ & I^+ s_\epsilon & I^+ s_\kappa \\ G^- & H^- & I^- s_\epsilon & I^- s_\kappa \end{bmatrix} \\ &\quad \times \begin{bmatrix} \delta\rho_1 \\ \delta\rho_2 \\ \delta\varphi \\ \delta\psi \end{bmatrix}. \end{aligned} \quad (\text{A2})$$

In Eq. (A2), $s_\epsilon = \epsilon \sin(\varphi^{\text{st}})$, $s_\kappa = \kappa \sin(\psi^{\text{st}})$, and c_ϵ and c_κ are defined in Eqs. (28) and (29) for both steady states.

Moreover, the parameters G^\pm , H^\pm , and I^\pm introduced in Eq. (A2) are determined as:

$$\begin{aligned} G^\pm &= -(c_\epsilon + c_\kappa) \left[1 \pm \beta_{12}^2 \right] \frac{1}{\varrho_2^{\text{st}}} + 2(\pm 2\beta_1 - \beta_c) \varrho_1^{\text{st}}, \\ H^\pm &= (c_\epsilon + c_\kappa) \left[\frac{1}{\beta_{12}^2} \pm 1 \right] \frac{1}{\varrho_1^{\text{st}}} - 2(2\beta_2 \mp \beta_c) \varrho_2^{\text{st}}, \\ I^\pm &= \frac{1}{\beta_{12}} \mp \beta_{12}. \end{aligned} \quad (\text{A3})$$

Whereas the dynamical matrix of deviations in Eq. (A1) can in general be diagonalized only numerically, analytical results are obtained in the case of \mathcal{PT} -symmetry ($\gamma_1 = -\gamma_2 \equiv -\gamma$, $\beta_1 = \beta_2 \equiv \beta$):

$$\varrho_1^{\text{st}} = \varrho_2^{\text{st}} = -(c_\epsilon + c_\kappa)/(2\beta + \beta_c),$$

$$\begin{aligned} s_\epsilon &= \gamma, \quad s_\kappa = 0, \\ |c_\epsilon| &= \sqrt{\epsilon^2 - \gamma^2}, \quad |c_\kappa| = \kappa. \end{aligned} \quad (\text{A4})$$

Writing the evolution of these deviations in the form $\exp(-i\tilde{\nu}_j t)$, the frequencies $\tilde{\nu}_j$ are obtained as follows:

$$\begin{aligned} \tilde{\nu}_{1,2} &= \pm 2i \sqrt{-c_\kappa(c_\epsilon + c_\kappa)}, \\ \tilde{\nu}_{3,4} &= \pm 2i \sqrt{-\frac{\beta c_\epsilon(c_\epsilon + c_\kappa)}{\beta + \beta_c/2}}, \end{aligned} \quad (\text{A5})$$

According to Eq. (A5), all $\tilde{\nu}_j$ are purely real for the steady state in Eq. (28) that lies at the border between the stable and unstable regions. On the other hand, just one out of four frequencies $\tilde{\nu}_j$ has a positive imaginary part, meaning the instability for the steady state in Eq. (29). Only if $c_\epsilon = -c_\kappa$, all four frequencies $\tilde{\nu}_j$ equal zero. This is the case of EPs.

-
- [1] C. M. Bender and S. Boettcher, “Real spectra in non-Hermitian Hamiltonians having \mathcal{PT} symmetry,” *Phys. Rev. Lett.* **80**, 5243–5246 (1998).
- [2] C. M. Bender, S. Boettcher, and P. N. Meisinger, “ \mathcal{PT} -symmetric quantum mechanics,” *J. Math. Phys.* **40**, 2201–2229 (1999).
- [3] C. M. Bender, D. C. Brody, and H. F. Jones, “Must a Hamiltonian be Hermitian?” *Am. J. Phys.* **71**, 1095–1102 (2003).
- [4] C. M. Bender, “Introduction to \mathcal{PT} -symmetric quantum theory,” *Contemp. Phys.* **46**, 277292 (2005).
- [5] R. El-Ganainy, K. G. Makris, D. N. Christodoulides, and Ziad H. Musslimani, “Theory of coupled optical \mathcal{PT} -symmetric structures,” *Opt. Lett.* **32**, 2632–2634 (2007).
- [6] H. Ramezani, T. Kottos, R. El-Ganainy, and D. N. Christodoulides, “Unidirectional nonlinear \mathcal{PT} -symmetric optical structures,” *Phys. Rev. A* **82**, 043803 (2010).
- [7] A. A. Zyablovsky, A. P. Vinogradov, A. A. Pukhov, A. V. Dorofeenko, and A. A. Lisiansky, “ \mathcal{PT} -symmetry in optics,” *Physics-Uspekhi* **57**, 1063–1082 (2014).
- [8] M. Öggen, F. K. Abdullaev, and V. V. Konotop, “Solitons in a \mathcal{PT} -symmetric $\chi^{(2)}$ coupler,” *Opt. Lett.* **42**, 4079–4082 (2017).
- [9] E. G. Turitsyna, I. V. Shadrivov, and Y. S. Kivshar, “Guided modes in non-Hermitian optical waveguides,” *Phys. Rev. A* **96**, 033824 (2017).
- [10] X. Xu, L. Shi, L. Ren, and X. Zhang, “Optical gradient forces in \mathcal{PT} -symmetric coupled-waveguide structures,” *Opt. Express* **26**, 10220–10229 (2018).
- [11] E.-M. Graefe and H. F. Jones, “ \mathcal{PT} -symmetric sinusoidal optical lattices at the symmetry-breaking threshold,” *Phys. Rev. A* **84**, 013818 (2011).
- [12] M.-A. Miri, A. Regensburger, U. Peschel, and D. N. Christodoulides, “Optical mesh lattices with \mathcal{PT} symmetry,” *Phys. Rev. A* **86**, 023807 (2012).
- [13] M. Ornigotti and A. Szameit, “Quasi \mathcal{PT} -symmetry in passive photonic lattices,” *J. Opt.* **16**, 065501 (2014).
- [14] T. Shui, W.-X. Yang, L. Li, and X. Wang, “Lop-sided Raman-Nath diffraction in \mathcal{PT} -antisymmetric atomic lattices,” *Opt. Lett.* **44**, 2089–2092 (2019).
- [15] B. Peng, Ş. K. Özdemir, F. Lei, F. Monifi, M. Gianfreda, G. L. Long, S. Fan, F. Nori, C. Bender, and L. Yang, “Parity–time-symmetric whispering-gallery microcavities,” *Nat. Phys.* **10**, 394–398 (2014).
- [16] B. Peng, Ş. K. Özdemir, S. Rotter, H. Yilmaz, M. Liertzer, F. Monifi, C. M. Bender, F. Nori, and L. Yang, “Loss-induced suppression and revival of lasing,” *Science* **346**, 328–332 (2014).
- [17] Z.-P. Liu, J. Zhang, S. K. Özdemir, B. Peng, H. Jing, X.-Y. Lü, C.-W. Li, L. Yang, F. Nori, and Y.-X. Liu, “Metrology with \mathcal{PT} -symmetric cavities: Enhanced sensitivity near the \mathcal{PT} -phase transition,” *Phys. Rev. Lett.* **117**, 110802 (2016).
- [18] X. Zhou and Y. D. Chong, “ \mathcal{PT} symmetry breaking and nonlinear optical isolation in coupled microcavities,” *Opt. Express* **24**, 6916–6930 (2016).
- [19] I. I. Arkhipov, A. Miranowicz, O. Di Stefano, R. Stassi, S. Savasta, F. Nori, and S. K. Özdemir, “Scully-Lamb quantum laser model for parity-time-symmetric whispering-gallery microcavities: Gain saturation effects and nonreciprocity,” *Phys. Rev. A* **99**, 053806 (2019).
- [20] F. Quijandría, U. Naether, S. K. Özdemir, F. Nori, and D. Zueco, “ \mathcal{PT} -symmetric circuit QED,” *Phys. Rev. A* **97**, 053846 (2018).
- [21] C. Tchodimou, P. Djourwe, and S. G. Nana Engo, “Distant entanglement enhanced in \mathcal{PT} -symmetric optomechanics,” *Phys. Rev. A* **96**, 033856 (2017).
- [22] D.-Y. Wang, C.-H. Bai, S. Liu, S. Zhang, and H.-F. Wang, “Distinguishing photon blockade in a \mathcal{PT} -symmetric optomechanical system,” *Phys. Rev. A* **99**, 043818 (2019).
- [23] A. Guo, G. J. Salamo, D. Duchesne, R. Morandotti, M. Volatier-Ravat, V. Aimez, G. A. Siviloglou, and D. N. Christodoulides, “Observation of \mathcal{PT} -symmetry breaking in complex optical potentials,” *Phys. Rev. Lett.* **103**, 093902 (2009).
- [24] R. El-Ganainy, M. Khajavikhan, and L. Ge, “Excep-

- tional points and lasing self-termination in photonic molecules,” *Phys. Rev. A* **90**, 013802 (2014).
- [25] W. Chen, Ş. Kaya Özdemir, G. Zhao, J. Wiersig, and L. Yang, “Exceptional points enhance sensing in an optical microcavity,” *Nature* **548**, 192–196 (2017).
- [26] J. Rubinstein, P. Sternberg, and Q. Ma, “Bifurcation diagram and pattern formation of phase slip centers in superconducting wires driven with electric currents,” *Phys. Rev. Lett.* **99**, 167003 (2007).
- [27] S. Bittner, B. Dietz, U. Günther, H. L. Harney, M. Miski-Oglu, A. Richter, and F. Schäfer, “ \mathcal{PT} symmetry and spontaneous symmetry breaking in a microwave billiard,” *Phys. Rev. Lett.* **108**, 024101 (2012).
- [28] X.-Y. Lü, H. Jing, J.-Y. Ma, and Y. Wu, “ \mathcal{PT} -symmetry-breaking chaos in optomechanics,” *Phys. Rev. Lett.* **114**, 253601 (2015).
- [29] T. T. Koutserimpas, A. Alù, and R. Fleury, “Parametric amplification and bidirectional invisibility in \mathcal{PT} -symmetric time-Floquet systems,” *Phys. Rev. A* **97**, 013839 (2018).
- [30] Ş. K. Özdemir, S. Rotter, F. Nori, and L. Yang, “Parity-time symmetry and exceptional points in photonics,” *Nat. Mat.* **18**, 783–798 (2019).
- [31] M. Miri and A. Alù, “Exceptional points in optics and photonics,” *Science* **363**, 7709 (2019).
- [32] G. S. Agarwal and K. Qu, “Spontaneous generation of photons in transmission of quantum fields in \mathcal{PT} -symmetric optical systems,” *Phys. Rev. A* **85**, 031802(R) (2012).
- [33] B. He, S.-B. Yan, J. Wang, and M. Xiao, “Quantum noise effects with Kerr-nonlinearity enhancement in coupled gain-loss waveguides,” *Phys. Rev. A* **91**, 053832 (2015).
- [34] S. Vashahri-Ghamsari, B. He, and M. Xiao, “Continuous-variable entanglement generation using a hybrid \mathcal{PT} -symmetric system,” *Phys. Rev. A* **96**, 033806 (2017).
- [35] S. Scheel and A. Szameit, “ \mathcal{PT} -symmetric photonic quantum systems with gain and loss do not exist,” *Eur. Phys. Lett.* **122**, 34001 (2018).
- [36] V. Peřinová, A. Lukš, and J. Křepelka, “Quantum description of a \mathcal{PT} -symmetric nonlinear directional coupler,” *J. Opt. Soc. Am. B* **36**, 855–861 (2019).
- [37] F. Minganti, A. Miranowicz, R. Chhajlany, and F. Nori, “Quantum exceptional points of non-Hermitian Hamiltonians and Liouvillians: The effects of quantum jumps,” e-print arXiv:1909.11619 (2019).
- [38] Q. Zhong, A. Ahmed, J. I. Dadap, R. M. Osgood Jr., and R. El-Ganainy, “Parametric amplification in quasi- \mathcal{PT} symmetric coupled waveguide structures,” *New J. Phys.* **18**, 125006 (2016).
- [39] D. A. Antonosyan, A. S. Solntsev, and A. A. Sukhorukov, “Photon-pair generation in a quadratically nonlinear parity-time symmetric coupler,” *Phot. Res.* **6**, A6–A9 (2018).
- [40] J. Naikoo, K. Thapliyal, S. Banerjee, and A. Pathak, “Quantum Zeno effect and nonclassicality in a \mathcal{PT} -symmetric system of coupled cavities,” *Phys. Rev. A* **99**, 023820 (2019).
- [41] S. Croke, “ \mathcal{PT} -symmetric Hamiltonians and their application in quantum information,” *Phys. Rev. A* **91**, 052113 (2015).
- [42] H. Hodaei, U. H. Absar, S. Wittek, H. Garcia-Gracia, R. El-Ganainy, D. N. Christodoulides, and M. Khajavikhan, “Enhanced sensitivity at higher-order exceptional points,” *Nature* **548**, 187 (2017).
- [43] M. Brandstetter, M. Liertzer, C. Deutsch, P. Klang, J. Schoberl, H. E. Tureci, G. Strasser, K. Unterrainer, and S. Rotter, “Reversing the pump dependence of a laser at an exceptional point,” *Nat. Commun.* **5**, 4034 (2014).
- [44] L. Chang, X. Jiang, S. Hua, C. Yang, J. Wen, L. Jiang, G. Li, G. Wang, and M. Xiao, “Parity-time symmetry and variable optical isolation in active-passive-coupled microresonators,” *Nat. Photon.* **8**, 524 (2014).
- [45] H. Jing, Ş. K. Özdemir, X.-Y. Lü, J. Zhang, L. Yang, and F. Nori, “ \mathcal{PT} -symmetric phonon laser,” *Phys. Rev. Lett.* **113**, 053604 (2014).
- [46] H. Lü, Ş. K. Özdemir, L. M. Kuang, F. Nori, and H. Jing, “Exceptional points in random-defect phonon lasers,” *Phys. Rev. App.* **8**, 044020 (2017).
- [47] Z. Lin, H. Ramezani, T. Eichelkraut, T. Kottos, H. Cao, and D. N. Christodoulides, “Unidirectional invisibility induced by \mathcal{PT} -symmetric periodic structures,” *Phys. Rev. Lett.* **106**, 213901 (2011).
- [48] A. Regensburger, C. Bersch, M.-A. Miri, G. Onishchukov, D. N. Christodoulides, and U. Peschel, “Parity-time synthetic photonic lattices,” *Nature* **488**, 167 (2012).
- [49] B. Peng, Ş. K. Özdemir, M. Liertzer, W. Chen, J. Kramer, H. Yilmaz, J. Wiersig, S. Rotter, and L. Yang, “Chiral modes and directional lasing at exceptional points,” *PNAS* **113**, 6845–6850 (2016).
- [50] L. Feng, Z. J. Wong, R.-M. Ma, Y. Wang, and X. Zhang, “Single-mode laser by parity-time symmetry breaking,” *Science* **346**, 972 (2014).
- [51] H. Hodaei, M.-A. Miri, M. Heinrich, D. N. Christodoulides, and M. Khajavikhan, “Parity-time-symmetric microring lasers,” *Science* **346**, 975 (2014).
- [52] J. Doppler, A. A. Mailybaev, J. Böhm, U. Kuhl, A. Girschik, F. Libisch, T. J. Milburn, P. Rabl, N. Moiseyev, and S. Rotter, “Dynamically encircling an exceptional point for asymmetric mode switching,” *Nature* **537**, 76–79 (2016).
- [53] H. Jing, Şahin K. Özdemir, Z. Geng, Jing Zhang, Xin-You Lü, Bo Peng, Lan Yang, and Franco Nori, “Optomechanically-induced transparency in parity-time-symmetric microresonators,” *Sci. Rep.* **5**, 9663 (2015).
- [54] H. Jing, Ş. K. Özdemir, H. Lü, and F. Nori, “High-order exceptional points in optomechanics,” *Sci. Rep.* **7**, 3386 (2017).
- [55] H. Benisty, A. Degiron, A. Lupu, A. De Lustrac, S. Chenaïs, S. Forget, M. Besbes, G. Barbillon, A. Bruyant, S. Blaize, and G. Lerondel, “Implementation of \mathcal{PT} symmetric devices using plasmonics: principle and applications,” *Opt. Express* **19**, 18004 (2011).
- [56] M. S. Tame, K. R. McEnery, Ş. K. Özdemir, J. Lee, S. A. Maier, and M. S. Kim, “Quantum plasmonics,” *Nat. Phys.* **9**, 329–340 (2013).
- [57] J. Schindler, A. Li, M.C. Zheng, F. M. Ellis, and T. Kottos, “Experimental study of active LRC circuits with \mathcal{PT} symmetries,” *Phys. Rev. A* **84**, 040101(R) (2011).
- [58] P.-Y. Chen and R. El-Ganainy, “Exceptional points enhance wireless readout,” *Nat. Electron.* **2**, 323–324

- (2019).
- [59] M. Kang, F. Liu, and J. Li, “Effective spontaneous \mathcal{PT} -symmetry breaking in hybridized metamaterials,” *Phys. Rev. A* **87**, 053824 (2013).
- [60] H. Xu, D. Mason, L. Jiang, and J. G. E. Harris, “Topological energy transfer in an optomechanical system with exceptional points,” *Nature* **537**, 80 (2016).
- [61] X. Zhu, H. Ramezani, C. Shi, J. Zhu, and X. Zhang, “ \mathcal{PT} -symmetric acoustics,” *Phys. Rev. X* **4**, 031042 (2014).
- [62] R. Fleury, D. Sounas, and A. Alù, “An invisible acoustic sensor based on parity-time symmetry,” *Nat. Commun.* **6**, 5905 (2015).
- [63] D. Leykam, K. Y. Bliokh, C. Huang, Y. D. Chong, and F. Nori, “Edge modes, degeneracies, and topological numbers in non-Hermitian systems,” *Phys. Rev. Lett.* **118**, 040401 (2017).
- [64] J. González and R. A. Molina, “Topological protection from exceptional points in Weyl and nodal-line semimetals,” *Phys. Rev. B* **96**, 045437 (2017).
- [65] W. Hu, H. Wang, P. P. Shum, and Y. D. Chong, “Exceptional points in a non-Hermitian topological pump,” *Phys. Rev. B* **95**, 184306 (2017).
- [66] T. Gao, G. Li, E. Estrecho, T. C. H. Liew, D. Comber-Todd, A. Nalitov, M. Steger, K. West, L. Pfeiffer, D. W. Snoke, A. V. Kavokin, A. G. Truscott, and E. A. Ostrovskaya, “Chiral modes at exceptional points in exciton-polariton quantum fluids,” *Phys. Rev. Lett.* **120**, 065301 (2018).
- [67] T. Liu, Y.-R. Zhang, Q. Ai, Z. Gong, K. Kawabata, M. Ueda, and F. Nori, “Second-order topological phases in non-Hermitian systems,” *Phys. Rev. Lett.* **122**, 076801 (2019).
- [68] K. Y. Bliokh, D. Leykam, M. Lein, and F. Nori, “Topological non-Hermitian origin of surface Maxwell waves,” *Nat. Commun.* **10**, 580 (2019).
- [69] M. Caspel, S. E. T. Arze, and I. P. Castillo, “Dynamical signatures of topological order in the driven-dissipative Kitaev chain,” *SciPost Phys.* **6**, 26 (2019).
- [70] Z.-Y. Ge, Y.-R. Zhang, T. Liu, S.-W. Li, H. Fan, and F. Nori, “Topological band theory for non-Hermitian systems from the Dirac equation,” *Phys. Rev. B* **100**, 054105 (2019).
- [71] H. Xu, D. Mason, Luyao Jiang, and J. G. E. Harris, “Topological energy transfer in an optomechanical system with exceptional points,” *Nature* **537**, 80–83 (2016).
- [72] J. D. H. Morales, J. Guerrero, S. López-Aguayo, and B. M. Rodríguez-Lara, “Revisiting the optical \mathcal{PT} -symmetric dimer,” *Symmetry* **8**, 83 (2016).
- [73] R. W. Boyd, *Nonlinear Optics* (Academic Press, New York, 2003).
- [74] L. Mandel and E. Wolf, *Optical Coherence and Quantum Optics* (Cambridge Univ. Press, Cambridge, 1995).
- [75] J. Peřina Jr. and J. Peřina, “Quantum statistics of nonlinear optical couplers,” in *Progress in Optics, Vol. 41*, edited by E. Wolf (Elsevier, Amsterdam, 2000) pp. 361–419.
- [76] F. A. A. El-Orany, M. S. Abdalla, and J. Peřina, “Quantum properties of the codirectional three-mode Kerr nonlinear coupler,” *Eur. Phys. J. D* **33**, 453–463 (2004).
- [77] K. Thapliyal, A. Pathak, B. Sen, and J. Peřina, “Higher-order nonclassicalities in a codirectional nonlinear optical coupler: Quantum entanglement, squeezing, and antibunching,” *Phys. Rev. A* **90**, 013808 (2014).
- [78] G. J. Milburn and C. A. Holmes, “Dissipative quantum and classical Liouville mechanics of the anharmonic oscillator,” *Phys. Rev. Lett.* **56**, 2237–2240 (1986).
- [79] G. J. Milburn and C. A. Holmes, “Quantum coherence and classical chaos in a pulsed parametric oscillator with a Kerr nonlinearity,” *Phys. Rev. A* **44**, 4704–4711 (1991).
- [80] A. Kowalewska-Kudłaszuk, J. K. Kalaga, and W. Leoński, “Wigner-function nonclassicality as indicator of quantum chaos,” *Phys. Rev. E* **78**, 066219 (2008).
- [81] A. Kowalewska-Kudłaszuk, J. K. Kalaga, and W. Leoński, “Long-time fidelity and chaos for a kicked nonlinear oscillator system,” *Phys. Lett. A* **373**, 1334–1340 (2009).
- [82] A. R. Shahinyan, L. Y. Chew, and G. Y. Kryuchkyan, “Probing quantum dissipative chaos using purity,” *Phys. Lett. A* **377**, 2743–2748 (2013).
- [83] W. Leoński and R. Tanaś, “Possibility of producing the one-photon state in a kicked cavity with a nonlinear Kerr medium,” *Phys. Rev. A* **49**, R20–R23 (1994).
- [84] A. Miranowicz and W. Leoński, “Two-mode optical state truncation and generation of maximally entangled states in pumped nonlinear couplers,” *J. Phys. B* **39**, 1683–1700 (2006).
- [85] G. H. Hovsepyan, A. R. Shahinyan, and G. Y. Kryuchkyan, “Multiphoton blockades in pulsed regimes beyond stationary limits,” *Phys. Rev. A* **90**, 013839 (2014).
- [86] A. Miranowicz, J. Bajer, M. Paprzycka, Y.-X. Liu, A. M. Zagoskin, and F. Nori, “State-dependent photon blockade via quantum-reservoir engineering,” *Phys. Rev. A* **90**, 033831 (2014).
- [87] A. Kowalewska-Kudłaszuk, W. Leoński, and J. Peřina Jr., “Generalized Bell states generation in a parametrically excited nonlinear coupler,” *Phys. Scr.* **T147**, 014016 (2012).
- [88] M. K. Olsen, “Asymmetric steering in coherent transport of atomic population with a three-well Bose-Hubbard model,” *J. Opt. Soc. Am. B* **32**, A15–A19 (2015).
- [89] M. K. Olsen, “Spreading of entanglement and steering along small Bose-Hubbard chains,” *Phys. Rev. A* **92**, 033627 (2015).
- [90] J. K. Kalaga, A. Kowalewska-Kudłaszuk, W. Leoński, and A. Barasiński, “Quantum correlations and entanglement in a model comprised of a short chain of nonlinear oscillators,” *Phys. Rev. A* **94**, 032304 (2016).
- [91] J. K. Kalaga, W. Leoński, and R. Szczyński, “Quantum steering and entanglement in three-mode triangle Bose-Hubbard system,” *Quant. Inf. Proc.* **16**, UNSP 265 (2017).
- [92] J. Peřina Jr., “Coherent light in intense spatio-spectral twin beams,” *Phys. Rev. A* **93**, 063857 (2016).
- [93] A. A. Sukhorukov, Z. Xu, and Y. S. Kivshar, “Nonlinear suppression of time reversals in \mathcal{PT} -symmetric optical couplers,” *Phys. Rev. A* **82**, 043818 (2010).
- [94] J. Peřina, *Quantum Statistics of Linear and Nonlinear Optical Phenomena* (Kluwer, Dordrecht, 1991).
- [95] M. Sargent, M. O. Scully, and W. E. Lamb, *Laser Physics* (Addison-Wesley, 1974).
- [96] P. Meystre and M. Sargent III, *Elements of Quantum Optics, 4th edition* (Springer, Berlin, 2007).

- [97] G. Adesso and F. Illuminati, “Entanglement in continuous variable systems: Recent advances and current perspectives,” *J. Phys. A: Math. Theor.* **40**, 7821–7880 (2007).
- [98] A. Lukš, V. Peřinová, and J. Peřina, “Principal squeezing of vacuum fluctuations,” *Opt. Commun.* **67**, 149—151 (1988).
- [99] J. Peřina Jr. and A. Lukš, “Quantum behavior of a \mathcal{PT} -symmetric two-mode system with cross-Kerr nonlinearity,” *Symmetry* **11**, 1020 (2019).
- [100] S. Hill and W. K. Wootters, “Entanglement of a pair of quantum bits,” *Phys. Rev. Lett.* **78**, 5022 (1997).